frontiers | Frontiers in Physics

TYPE Brief Research Report
PUBLISHED 12 January 2023
DOI 10.3389/fphy.2022.1115447

OPEN ACCESS

EDITED BY
Zhenxu Bai,
Hebei University of Technology, China

REVIEWED BY
Jianglin Zou,
Beijing University of Technology, China
Xiaorong Guan,
Nanjing University of Science and Technology, China

*CORRESPONDENCE
Pengjun Zhang,
zhangpj@nuc.edu.cn

SPECIALTY SECTION
This article was submitted to Optics and Photonics, a section of the journal Frontiers in Physics

RECEIVED 04 December 2022
ACCEPTED 28 December 2022
PUBLISHED 12 January 2023

CITATION
Ren D, Zhang P, Yu J, Yao Y and Li X (2023), Study on the quenching depth and surface hardness of metal materials by laser quenching variable parameters.
Front. Phys. 10:1115447.
doi: 10.3389/fphy.2022.1115447

Study on the quenching depth and surface hardness of metal materials by laser quenching variable parameters

Dongdong Ren[1], Pengjun Zhang[1]*, Jiahui Yu[1], Yangwu Yao[1] and Xiaoyang Li[2]

[1]School of Mechatronics Engineering, North University of China, Taiyuan, China, [2]Military and Political Training Department, Shijiazhuang Division of PLAA Infantry Academy, Shijiazhuang, China

Laser quenching is one of the most outstanding gear tooth surface quenching methods due to its high efficiency, environmental friendliness, and performance consistency. Since gear tooth surface laser quenching requires repeated scanning, changing the laser scanning velocity and power by program control can meet the needs of variable depth quenching. The effects of laser scanning velocity and output power on the quenching depth and surface Rockwell hardness after quenching were studied and experimentally analyzed. The result shows that by adjusting the parameters, the surface hardness of the specimen changes slightly with the actual received laser energy. However, the quenching depth can be consistent with the laser scanning velocity. The maximum surface Rockwell hardness that a laser quenched material can achieve depends on the material itself, not on the laser power or scanning velocity. Compared with accelerated laser quenching, decelerated laser quenching is more suitable for tooth surface machining due to the cumulative effect of energy within the quenching depth range of metal materials.

KEYWORDS

laser quenching, quenching depth, Rockwell hardness, scanning velocity, dimensionless power

1 Application introduction

High-frequency laser quenching is a technology widely used in the heat treatment process of metal materials, which is an effective method to improve the mechanical properties of steel with high carbon content [1, 2]. Feng [3] studied the microstructure and mechanical properties of composite strengthened high chromium cast iron by laser quenching and laser shock processing. The microstructure observation, microhardness, residual stress and full width at half maximum (FWHM) measurement, impact toughness, and wear experiment were carried out on untreated, laser quenched, and laser quenched-laser shock peening high chromium cast iron samples. Tang [4] adopted a new laser induction hybrid quenching process, combined with laser and electromagnetic induction heat source, to improve the depth and uniformity of the laser hardening layer of 42CrMo steel. Li [5] established a combination of temperature and microstructure prediction models for laser quenching of GCr15 bearing steel. Based on the experimental results, the temperature and microstructure evolution of GCr15 bearing steel during laser quenching were simulated. YasudaT [6] characterized the nanomechanics and sub-microstructure of laser quenching-induced heat-affected zone (HAZ) of carbon steel.

The mechanical properties of the samples were characterized by nanoindentation, and the microstructure was observed by using a scanning electron microscope (SEM).

The gear transmission system relies on the meshing contact of the gear tooth surface to transmit power. One of the biggest influencing factors of the non-linear dynamic characteristics of the system is the dynamic meshing stiffness. One of the factors affecting the dynamic meshing stiffness of the gear system is the local material stiffness of the meshing area of the tooth surface, which is determined by the surface hardness of the material and the characteristics of the shallow structure. At present, laser quenching is one of the most environment friendly and easy-to-control process quality among several gear tooth surface quenching technologies, which has the highest consistency of mechanical properties after quenching. Related physical and chemical mechanisms and processing equipment and technology are constantly being widely studied and applied. Surface hardening heat treatment is widely used to improve tooth surface properties such as wear and rolling contact fatigue [7, 8]. After the experiment, Cai [9] found that the cracks mainly appeared in the top fillet, pitch circle, and tooth root of the gear. The size and distribution of slag inclusions in 16MnCr5 steel also had a certain influence on the origin of gear surface cracks. Barglik, J [10] measured the microstructure of gears by continuous dual-frequency induction hardening of small gears made of special quality steel AISI 4340. Li [11] studied the quenching microstructure and hardness distribution of 40Cr gear steel by means of a Axioskop 2 scanning electron microscope, KEYENCE VH-Z100R ultra-depth 3D microscope, and Q10M microhardness experimenter and revealed the mechanical behavior and phase hardening law of the material during quenching.

In general, in the application of the processing industry, the high consistency of the mechanical performance of the products is guaranteed by the initial settings of the laser, such as source power, wavelength, and other parameters. Therefore, many studies have been carried out based on invariant laser source characteristic parameters [12]. In this paper, several laser light source parameters that can be automatically adjusted by the laser control system are selected, and their changes in the mechanical properties of the gear tooth surface after quenching are experimented and studied. Considering that the laser quenching technology is applied to gear tooth surface quenching with a modulus more than 5, the results will be excellent. Therefore, we focus on the laser light source power, scanning velocity, and scanning frequency to analyze the tooth surface quenching depth and Rockwell hardness. At the same time, in order to obtain more accurate numerical results in the experiment, the laser quenching experiment was carried out by using the method of plane specimen and laser vertical scanning in the process of controlling the experiment variables.

2 Theoretical analysis of laser quenching

Laser scanning quenching used in this paper is a directional transmission of heat by transforming a cylindrical laser beam passing through a set of zoom field lens into a fan-shaped beam illuminating the target surface, and then, a local heating layer is formed on the surface of the material. The heat conduction from the high-temperature surface of the material to the substrate is the main heat transfer mode of laser quenching, and it is also the key to phase transformation hardening during laser quenching. Laser quenching phase transformation hardening can obtain higher residual compressive stress on the surface, which is determined by the characteristics of laser quenching local treatment.

As the material cools, the structure changes and its unit volume also changes, resulting in an increase in the volume of the material and an increase in compressive stress, and the direction of this structural transformation is opposite to the direction of heat conduction, that is, the inner layer points to the surface of the material. Therefore, the volume of the material's structural transformation increases, causing the compressive stress to expand from the inner layer to the surface, resulting in a hardened layer with a high residual compressive stress in the hardened layer. The local rapid heating and cooling make the ultra-fine grain austenite of the steel grow very late, and the martensite structure after laser phase transformation strengthening becomes very fine lath martensite and contracture martensite to obtain an ultra-fine grain size and phase transformation structure. The line scanning laser and its gear quenching principle and basic working mode are shown in Figure 1.

As shown in Figure 1, the scanning laser is protected by the CO_2 shielding gas flow, which is emitted from the laser equipment output after passing through the zoom field lens and directly irradiated on the surface of the gear teeth. After irradiation, an elliptical spot is formed on the surface of the gear. The power of the laser energy emitted by the laser during operation and transmitted to the surface of the target material is derived as follows:

$$P_L = P/\eta = Q\frac{\pi ab}{2\eta\eta_0}\cdot \exp\left[-2\cdot\frac{x^2+(y-v\cdot t)^2}{ab}\right]^{-1}, \tag{1}$$

where P_L is the laser source power, η is the laser source emission efficiency, Q is the laser energy density, η_0 is the laser quenching energy efficiency, a and b are the spot half-axis length on the x and y axes, respectively, and v is the laser scanning velocity.

According to the change mechanism of the laser absorption rate, the laser absorption rate of the steel alloys will gradually increase with the increase of its own resistivity [13]. The relationship is as follows:

$$A = 0.1457\sqrt{\frac{\rho}{\lambda}} + 0.09e^{-0.5\sqrt{\frac{\lambda\cdot\frac{c}{N}}{\rho}}} + \frac{\rho}{N\lambda - 10^{-6}}, \tag{2}$$

where A is the laser absorption rate, ρ is the resistivity of the material, N is the number of electrons outside the material, λ is the laser wavelength, and c is a fixed constant.

For a more accurate analysis of the relationship between the laser source and the quenching properties, the output power of the source and the actual laser energy received by the surface of the quenched object need to be accurately quantified. The change of energy in the interaction between the laser and the metal material follows the energy conservation equation:

$$E_0 = E_r + E_a + E_t, \tag{3}$$

where E_0 is the laser energy incident on the surface of the material, E_r is the energy reflected by the material, E_a is the energy absorbed by the material, and E_t is the energy retained after the laser passes through the material.

Eq. 3 can be transformed into the following equation:

$$1 = \frac{E_r}{E_0} + \frac{E_a}{E_0} + \frac{E_t}{E_0} = R + \alpha + T, \tag{4}$$

where R is the reflection coefficient, α is the absorption coefficient, and T is the transmission coefficient.

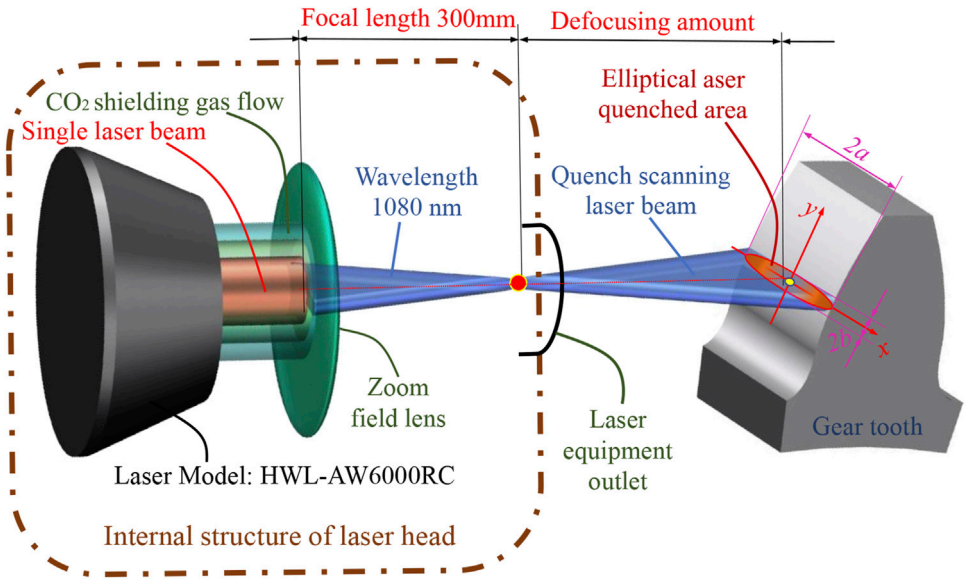

FIGURE 1
Variable depth quenching principle of gears by laser quenching.

During high-power laser quenching, the heat transfers to the surface of the steel instantaneously, so this causes the surface temperature to accumulate rapidly and rises to the critical point of phase transformation of the steel and continues to rise. As soon as laser scanning is completed, the heat in this region is rapidly transferred to the metal matrix, and the rapid decrease of temperature leads to the rapid conversion of some austenite structures into martensite. The carbon element in the retained austenite cannot diffuse, resulting in an increase in the carbon content of the martensite, thus resulting in an increase in the hardness of the region after laser scanning. Using the energy balance of the solid–liquid interface as the detection criterion of interface motion, the mathematical model for predicting and controlling the tissue under rapid solidification conditions is as follows [14]:

$$\mu = (2B - B - a) + \left[(2B - B - a)^2 - b\right]^{1/2}. \tag{5}$$

In the equation,

$$\begin{cases} a = (1-k)\varepsilon/(k+V), \\ 2B = \dfrac{aV}{1+V} + \dfrac{1-k}{1+k}, \\ b = \dfrac{a(a+V+k)}{1+V}, \\ V = \delta_i/D_i, \end{cases} \tag{6}$$

where k is the equilibrium distribution coefficient, δ_i is the jump distance between atoms, D_i is the interface diffusion coefficient, V is the velocity constant obtained by the solid–liquid interface when the molten pool reaches the quasi-steady state, and ε is the dimensionless concentration coefficient of the interface temperature. In the three cases of steady state ($\mu < 0$), the corresponding structures formed by rapid solidification are the planar crystal structure, cellular crystal structure, ($\mu = 0$) and dendritic structure ($\mu > 0$).

For the isothermal kinetic model of diffusive phase transition [15], the basic form is as follows:

$$f_{(T,t)} = 1 - \exp[-bt^n], \tag{7}$$

where $f_{(T,t)}$ is the amount of the new phase, t is the time, and b and n are the material constants under certain conditions.

For non-diffusion martensitic transformation, the amount of transformation is only determined by temperature and has nothing to do with time. The martensitic transformation formula can be expressed as follows [16]:

$$f_m = f^*\left(1 - \left(\frac{T - M_f}{M_s - M_f}\right)^{2.5}\right), \tag{8}$$

where T is the current temperature, M_s is the starting temperature of martensitic transformation, M_f is the termination temperature of martensitic transformation, and f_m is the martensite content.

According to the aforementioned analysis, when we use high-power laser quenching equipment to quench the surface layer of the gear tooth surface, we can analyze the actual quenching effect of laser quenching on steel by the quenching experiment of different laser light source power and frequencies, scanning spot sizes, and scanning velocities (quenching depth and surface Rockwell hardness). In addition, the effect of laser scanning velocity on the mechanical properties of steel was studied. In order to eliminate the influence of the gear tooth profile radian on the laser scanning velocity and angle and, at the same time, to ensure the single variable principle of the experiment and control the variable accuracy in the experiment process, we used cuboid specimens for experimenting. As a widely used material, the experimental results of 45 steel would be highly representative. Its high carbon content could also show the mechanical performance change suitability during laser quenching, so it is used as the target material of our experiment specimens.

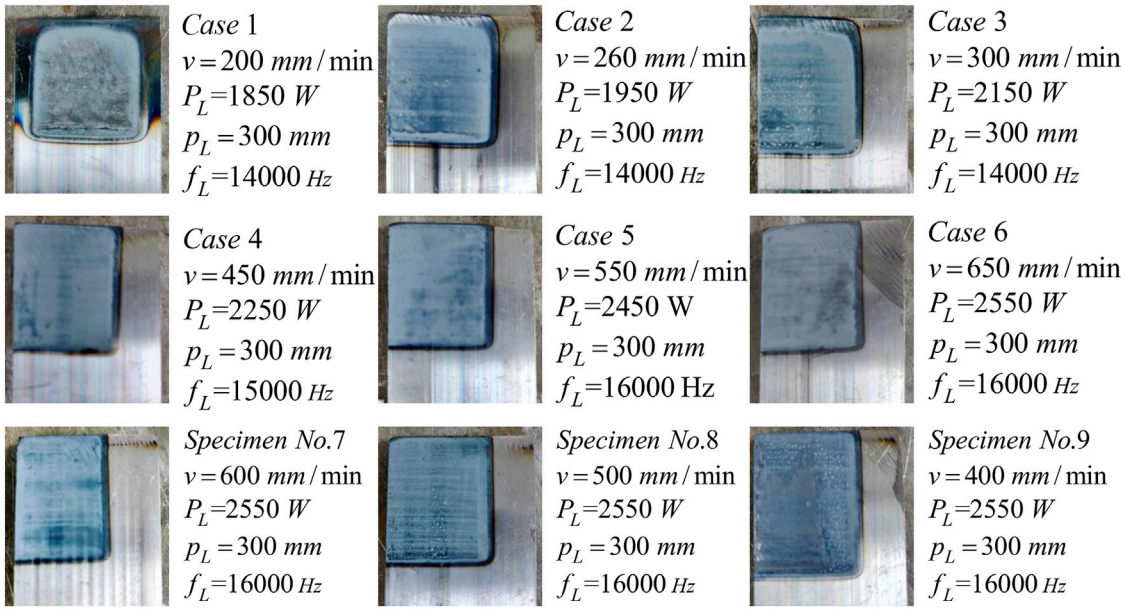

FIGURE 2
Actual morphology of 9 specimens after laser quenching.

TABLE 1 Results of the laser quenching depth and surface hardness.

Parameter	Case 1	Case 2	Case 3	Case 4	Case 5	Case 6	Case 7	Case 8	Case 9
Scanning velocity (mm/min)	200	250	300	450	550	650	600	500	400
Laser power(W)	1850	1950	2100	2250	2400	2550	2550	2550	2550
Laser focus (mm)	300	300	300	300	300	300	300	300	300
Depth of quenching (mm)	0.90	0.80	0.60	0.50	0.40	0.40	0.55	0.80	0.90
Rockwell hardness (HRC)	60	58	61	54	58	55	61	61	61

3 Experimental process

In order to obtain reasonable experiment results, this paper uses HWL-AW6000RC laser quenching equipment which can stably control the high-power output parameters of the laser to experiment the laser quenching treatment of the surface of 45 steel specimens. The maximum power of this type of laser equipment is 6000 W, and the actual output power of the laser source can reach 3000 W. The laser beam is a single beam, and the scanning range is 0–30 mm. During the experiment, laser focal length is fixed (300 mm) and the laser scanning width is 20 mm, which is slightly less than the width of the specimen.

The material of the experiment specimen is 45 steel, and the size of each specimen is 30 × 20 × 5 mm. Before the experiment, the surface roughness of each sample was uniformly treated and cleaned with alcohol. The experiment was divided into three groups. The first group was quenched with stable velocity, including 27 cases. The second group was subjected to an accelerated quenching experiment, including 12 cases. The third group conducted a deceleration experiment, including 12 cases. In the first group, nine well-behaved specimens were taken as reference and the average surface Rockwell hardness was experimented. Finally, the actual quenching depth is measured after the experiment, and the average Rockwell hardness and quenching depth are determined at three positions for the other two specimens. After the preliminary selection and trial analysis of the laser light source and quenching parameters, we selected the following parameters for formal experiment analysis.

In this laser quenching experiment group, nine qualified samples in the first group were selected for display. Figure 2 shows the actual morphology and their different parameters after laser quenching.

It can be known from the laser quenching experiment results that the surface consistency of the quenching experiment at a fixed laser scanning velocity is consistent, and the results under the same experiment conditions are basically consistent identically.

Based on this result, we determine that the laser quenching power and frequency used in variable velocity laser quenching as follows are consistent with cases 7, 8, and 9.

After experimenting with the surface Rockwell hardness of the cases, we cut the specimens longitudinally without damage and

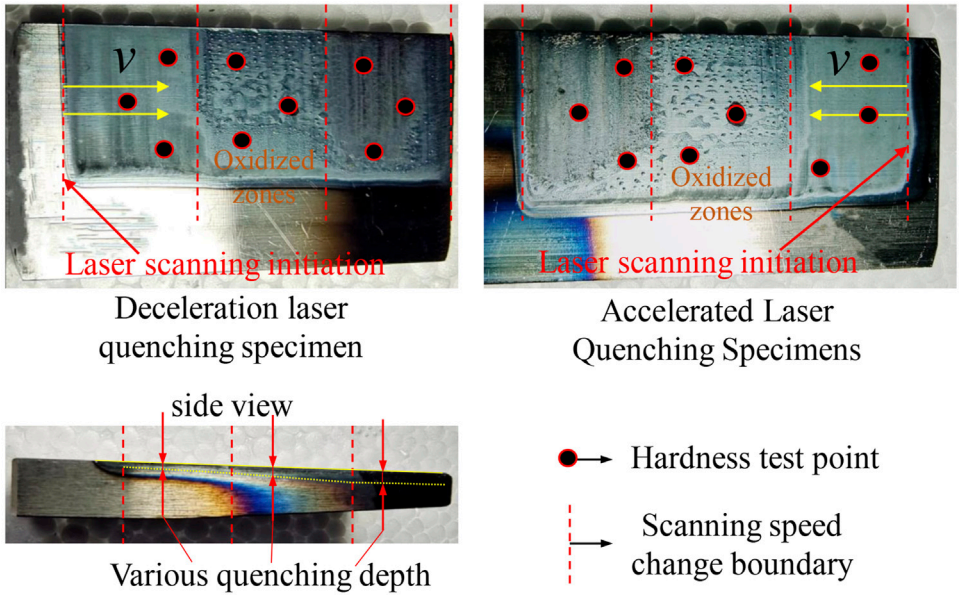

FIGURE 3
Schematic diagram of specimen morphology after accelerated and decelerated laser quenching.

TABLE 2 Dimensionless results of variable quenching parameters.

	Case 1	Case 2	Case 3	Case 4	Case 5	Case 6	Case 7	Case 8	Case 9	Case 10	Case 11
Dimensionless energy	3.92	4.08	4.25	4.43	4.63	4.85	5.10	5.37	5.67	6.00	6.38
Dimensionless depth (velocity increase)	4.0	5.0	5.8	6.5	7.0	7.5	8.1	8.45	8.6	8.85	9.0
Dimensionless depth (velocity decrease)	4.0	5.0	5.7	6.7	7.2	7.5	8.1	8.6	8.8	8.9	9.0

measured the actual quenching depth. The laser quenching depth and surface Rockwell hardness of every case as a reference for the further experiment are shown in Table 1.

The Rockwell hardness experiment of steel specimen material before laser quenching is 30HRC. Comparing the results in the aforementioned table, it can be found that high-power and high-frequency laser scanning quenching can quickly increase the surface hardness of the material with a thickness of 1 mm. But for 45 steel, on the surface layer within 1 mm after laser quenching, its Rockwell hardness can only reach 61HRC, which is related to its material composition. In addition, according to the aforementioned experiment results and empirical analysis, the laser light source power and quenching scanning velocity are the most important parameters affecting the material properties after quenching.

The laser scanning velocity changes in both accelerated and decelerated laser quenching experiments (scanning velocity varies from 400 to 650 mm/min). The scanning velocity is smoothly changed by the automatic control system of the laser itself. The experiment process was carried out at standard room temperature. At the same time, the laser quenching process was only protected by the CO_2 protective gas of the laser itself, and different degrees of spotted oxidation zones appeared in the intermediate variable velocity stage of the laser quenching specimen. However, after the hardness experiment, we find that spotted oxidation zones had little effect on the surface hardness of the specimen. The morphology of comparative specimens after accelerated and decelerated laser quenching is shown in Figure 3.

It can be seen from the aforementioned figure that the variable velocity laser quenching process shows little difference in morphology, and the quenching area and boundary area of the material surface after laser quenching still maintain a high surface quality.

On the side view of the uncut section, it can be seen that the quenching layer at the edge of the specimen is also consistent with the variation of the scanning velocity. It can be seen that the quenching scheme of automatic control of scanning velocity by the laser quenching system can meet the process requirements of variable depth and surface hardness. In addition, because the surface of the specimen is not protected by inert gas during the quenching process, the morphology of the intermediate variable velocity region of the laser quenching of the specimen shows a certain amount of spotted oxidation zones, which may be due to the unstable quenching velocity.

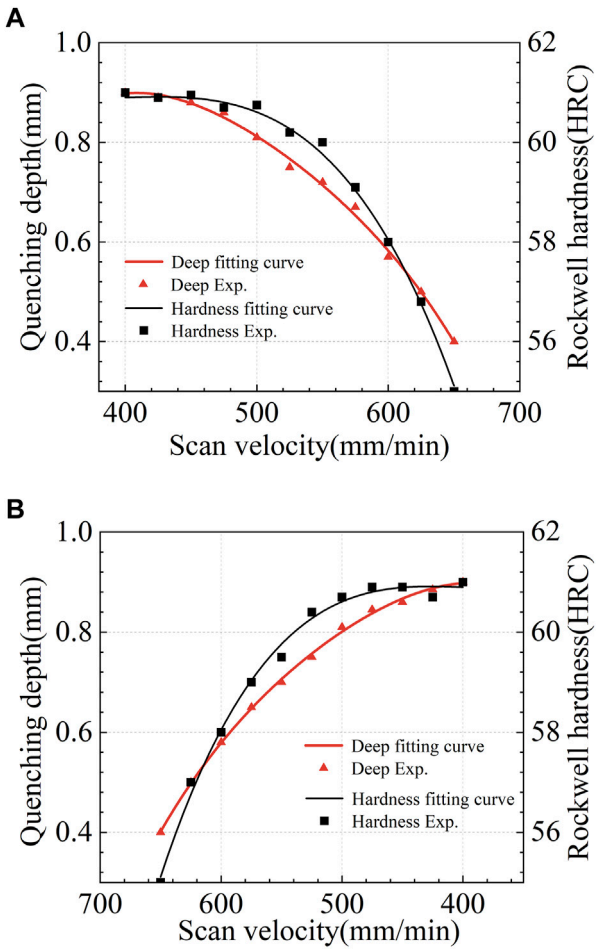

FIGURE 4
(A) Deceleration quenching results. **(B)** Accelerated quenching results. Results of variable quenching scanning velocity.

4 Results and discussion

After completing all the experiment cases, we performed Rockwell hardness experiments on the surface of specimens quenched by a variable velocity laser. The specimen was then subjected to a non-destructive longitudinal cutting to measure its actual quenching depth. The measurement results of the second group of specimens are averaged, and the distribution results are interpolated by multiple term functions to obtain the fitting results, as shown in Figure 4.

As it is shown in Figure 4A, during the scanning process of deceleration laser quenching, the actual quenching depth of the specimen is basically consistent with the reference specimen, and the average hardness is basically consistent with the reference specimen in the initial stage, but it tends to the maximum value and remains stable in the final stage of deceleration.

It can be seen from Figure 4B that during the scanning process of decelerated laser quenching, the actual quenching depth of the specimen is basically consistent with that of the reference specimen, while the hardness is basically consistent with the result of the reference specimen in the initial stage of acceleration. However, in the final stage of acceleration, there is a slight change and its value decreases slightly faster.

From the previous numerical analysis, it can be seen that whether it is accelerated or decelerated scanning; the effect of laser quenching on the surface Rockwell hardness of 45 steel is consistent with that of constant velocity scanning. The reason is that despite the high frequency and high-power laser quenching used in the experiment, the energy transfer efficiency is sufficient to meet the energy demand of the phase change of the material surface structure in a short time, but the increase of hardness depends on the specific composition of the structure, especially the carbon content level. However, during variable speed quenching in a short time, the accumulative effect of laser energy on the surface of the material and the temperature rise of the shallow layer of the material are different, resulting in a slight difference in the final quenching performance.

Then, we numerically analyzed the actual output power of the dimensionless laser and the average quenching depth of the variable velocity scanning quenching specimen, ignoring the effect of laser scanning time. The results are shown in Table 2.

According to Table 2, when the influence of the heat accumulation effect caused by scanning time on the quenching depth is not considered (that is, when the influence of the scanning velocity is not considered), the laser source power in the laser quenching process is almost proportional to the actual quenching depth because the higher the laser output power in unit time, the more heat the material receives, resulting in a rapid temperature rise and faster radiation to the deep material.

Although the output power and scanning velocity of the laser source have a major impact on the actual effect of quenching, the program control adjustment of the scanning velocity can change the quenching performance within a certain range when the laser power is inconvenient to change in production applications. Coincidentally, for a commonly used small gear with the modulus about 5–10, the laser scanning velocity adjustment range can be applied to their tooth surface quenching depth changes. However, according to [17] and Equations 4, 8, the maximum hardness of metal materials achieved by laser quenching is related to the material itself. Therefore, in practical applications, when the same material is quenched to a specified depth using variable parameter laser parameters, its final performance can be determined by dimensionless laser scanning speed and power.

5 Conclusion

Variable velocity laser quenching is one of the most effective methods to precisely control the variable depth quenching process of the gear tooth surface, compared with other quenching techniques and control methods. Although laser quenching has excellent consistency and controllability compared to other quenching techniques, we do not recommend changing the scanning velocity too fast to avoid other uncontrollable damage on the surface of the specimen during laser quenching without inert gas protection. For further summary, we have the following conclusions.

1) The quenching experiment of 45 steel with fixed focus was carried out by changing the laser scanning velocity. It was found that the change of the laser quenching depth with the laser scanning velocity can be controlled within a reasonable range, and the surface hardness of the quenched sample also meets the expectation with an increase in percentage from 80% to 100%.
2) By adjusting the parameters of the laser source power and the scanning velocity for quenching experiments, we found that the

surface hardness of the specimen does not change with the excessive laser energy received in fact. The reason is that the microstructure characteristics of the alloy at a given quenching depth, especially the carbon content, determine its maximum hardness level.

3) Taking constant velocity laser quenching as a reference, the Rockwell hardness of the specimens after accelerated and decelerated laser quenching is taken into consideration and analyzed. Compared to the results of material properties under two experiment conditions, it is found that the rate characteristics of heat accumulation effect deceleration quenching may be more suitable for laser quenching of the gear surface with increased laser quenching depth.

Data availability statement

The original contributions presented in the study are included in the article/supplementary material; further inquiries can be directed to the corresponding author.

Author contributions

DR proposed the idea of this paper, finished the formulation and implementation of the research content and experiment program, and then completed the main writing of the manuscript. PZ investigated and sorted out the application of laser equipment and the related literature studied in this paper, and undertook the manuscript collation and submission process. JY carried out the experimental implementation process and operated the experiment data collection, screening, and statistical analysis in this paper. YY analyzed the mechanism and application background of laser quenching for strengthening the mechanical properties of alloy materials. In addition, YY provided a correction for the research direction and technical route of this paper. XL provided the materials' parameter data for the experiment process and the mechanical performance analysis device.

Funding

This study was funded by the Pre-Researching Key Project of National Defense: 208052020305.

Acknowledgments

The authors thank Dongguan Huawei Laser Equipment Co., Ltd., for their full support of laser quenching equipment and experimenting provided for this paper. The authors declare that this study received contribution from Huawei Laser Equipment Co., Ltd. The company was not involved in the study design, collection, analysis, interpretation of data, the writing of this article or the decision to submit it for publication.

Conflict of interest

The authors declare that the research was conducted in the absence of any commercial or financial relationships that could be construed as a potential conflict of interest.

Publisher's note

All claims expressed in this article are solely those of the authors and do not necessarily represent those of their affiliated organizations, or those of the publisher, the editors, and the reviewers. Any product that may be evaluated in this article, or claim that may be made by its manufacturer, is not guaranteed or endorsed by the publisher.

References

1. Zhang W, Yang S, Lin Z, Tao W. Weld morphology and mechanical properties in laser spot welding of quenching and partitioning 980 steel. *J Manufacturing Process* (2020) 56: 1136–45. doi:10.1016/j.jmapro.2020.05.057

2. Biungxu W, Yuming P, Yu L, Lyu N, Barber GC, Wang R, et al. Effects of quench-tempering and laser hardening treatment on wear resistance of gray cast iron. *J Mater Res Tech* (2020) 9(4):8163–71. doi:10.1016/j.jmrt.2020.05.006

3. Feng A, Wei Y, Liu B, Chen C, Pan X, Xue J. Microstructure and mechanical properties of composite strengthened high-chromium cast iron by laser quenching and laser shock peening. *J Mater Res Tech* (2022) 20:4342–55. doi:10.1016/j.jmrt.2022.08.148

4. Zehao T, Qunli Z, Hua H, Zhijun C, Junsheng C, Jianhua Y. Geometric characteristics and microstructure of laser-induction hybrid quenching hardened layer on 42CrMo steel. *Rare Metal Mater Eng* (2022) 51(7):2519–28.

5. Li Z, Wen Z, Su F. Modeling research on laser quenching process of GCr15 bearing steel basing on material properties obtained with experimental methods. *Mater Res Express* (2021) 8(9):096516. doi:10.1088/2053-1591/ac2341

6. Yasuda T, Shozui R, Nishimoto K, okumoto Y, Ohmura T. Nano-mechanical and sub-micro-structural characterization of spot-laser-quenched carbon steel[J]. *Tetsu Hagane-Journal Iron Steel Inst Jpn* (2022) 108(7):405–23. doi:10.2355/tetsutohagane.TETSU-2021-090

7. Sugimoto T, Ju DY. Influence of thermal boundary conditions on the results of heat treatment simulation. *Mater Trans* (2018) 59:950–6. H-M2018816. doi:10.2320/matertrans.H-M2018816

8. Su Y, Oikawa K, Shinohara T, Kai T, Horino T, Idohara O, et al. Neutron Bragg-edge transmission imaging for microstructure and residual strain in induction hardened gears. *Scientific Rep* (2021) 11(1):4155–14. doi:10.1038/s41598-021-83555-9

9. Cai S, Sun J, He Q, Shi T, Wang D, Si J, et al. 16MnCr5 gear shaft fracture caused by inclusions and heat treatment process. *Eng Fail Anal* (2021) 126:105458. doi:10.1016/j.engfailanal.2021.105458

10. Barglik J, Ducki K, Kuc D, Smagor A, Smalcerz A. Hardness and microstructure distributions in gear wheels made of steel AISI 4340 after consecutive dual frequency induction hardening. *Int J Appl Electromagnetics Mech* (2020) 63(S1):S131–40. doi:10.3233/jae-209111

11. Li C, Gao H, Chen X, Liu Z, Han X. Study on multi-field coupled evolution mechanism of laser irradiated 40Cr steel quenching process based on phase change induced plasticity. *Met Mater Int* (2022) 28(8):1919–37. doi:10.1007/s12540-021-01093-5

12. Muthukumaran G, Dinesh Babu P. Laser transformation hardening of various steel grades using different laser types. *J Braz Soc Mech Sci Eng* (2021) 43(2):103–29. doi:10.1007/s40430-021-02854-4

13. Jun C, Qunli Z, Jianhua Y, Jibin F. Laser absorptivity of metallic materials [J]. *Appl Opt* (2008)(05) 793–8.

14. Guo W, Kar A. Interfacial instability and microstructural growth due to rapid solidification in laser processing. *Acta Materialia* (1998) 46(10):3485–90. doi:10.1016/s1359-6454(98)00050-0

15. Avrami M. Kinetics of phase change. I general theory. *J Chem Phys* (1939) 7(12): 1103–12. doi:10.1063/1.1750380

16. Koistinen DP, Marburger R. A general equation prescribing the extent of the austenite-martensite transformation in pure iron-carbon alloys and plain carbon steels. *Acta metallurgica* (1959) 7:59–60. doi:10.1016/0001-6160(59)90170-1

17. Ibrahim MZ, Sarhan AAD, Kuo TY, Yusof F, Hamdi M. Characterization and hardness enhancement of amorphous Fe-based metallic glass laser cladded on nickel-free stainless steel for biomedical implant application. *Mater Chem Phys* (2019) 235:121745. doi:10.1016/j.matchemphys.2019.121745